

Optimization and Comparison of $\text{Al}_{0.2}\text{Ga}_{0.8}\text{As}$ and $\text{Ga}_{0.51}\text{In}_{0.49}\text{P}$ Window Layers for Single-Junction GaAs Solar Cell Using PC1D Simulation

Emile Philogias Rasoloniaina¹; Pr. Elisée Rastefano²

^{1,2}EAD SE-I-SMDE, ED-STII, Antananarivo, Madagascar

Publication Date: 2025/08/23

Abstract: Window layer plays a crucial role in enhancing solar cells efficiency. GaAs-based solar cells are widely recognized for their high efficiencies. This high performance can be attributed to the availability of various materials suitable for window layers. Numerical simulation can be used to identify the best among those materials. The aim of this work is to optimize and then compare two well-known window layer materials for GaAs-based solar cells: $\text{Al}_{0.2}\text{Ga}_{0.8}\text{As}$ and $\text{Ga}_{0.51}\text{In}_{0.49}\text{P}$, using PC1D simulation. The simulation results indicate that $\text{Ga}_{0.51}\text{In}_{0.49}\text{P}$ is more suitable for GaAs-based solar cells, demonstrating a higher open-circuit voltage, higher fill factor, and higher maximal power output. These better results are due to superior optical properties of $\text{Ga}_{0.51}\text{In}_{0.49}\text{P}$.

Keywords: Efficiency Improvement, Gaas-Based Solar Cell, PC1D Simulation, Window Layer, III-V Semiconductors, Surface Passivation.

How to Cite: Emile Philogias Rasoloniaina; Pr. Elisée Rastefano (2025) Optimization and Comparison of $\text{Al}_{0.2}\text{Ga}_{0.8}\text{As}$ and $\text{Ga}_{0.51}\text{In}_{0.49}\text{P}$ Window Layers for Single-Junction GaAs Solar Cell Using PC1D Simulation. *International Journal of Innovative Science and Research Technology*, 10(8), 947-958. <https://doi.org/10.38124/ijisrt/25aug786>

I. INTRODUCTION

The pursuit of sustainable solutions to accommodate the increasing global energy demand, particularly in the context of global warming, has become a primary focus for researchers in the renewable energy field. Solar energy stands as one of the most economically viable options to reduce our reliance on fossil fuels. The journey started with silicon-based photovoltaics, which provided a source of low-cost, clean energy. However, silicon photovoltaics have now reached their Shockley-Queisser limit, which has led researchers to

explore the use of III-V compound materials such as Gallium Arsenide (GaAs), Indium Phosphide (InP), Aluminum Gallium Arsenide (AlGaAs) and Indium Gallium Phosphide (InGaP). These III-V compound materials boast a high absorption coefficient due to their direct bandgap, and they exhibit higher resistance to photon radiations, making them suitable for space applications. Reference [1] has illustrated with Fig. 1 the historical and projected efficiency for III-V single-junction solar cells. As shown, GaAs exhibits the highest efficiency under 1-sun condition, thereby explaining the concentrated focus on GaAs.

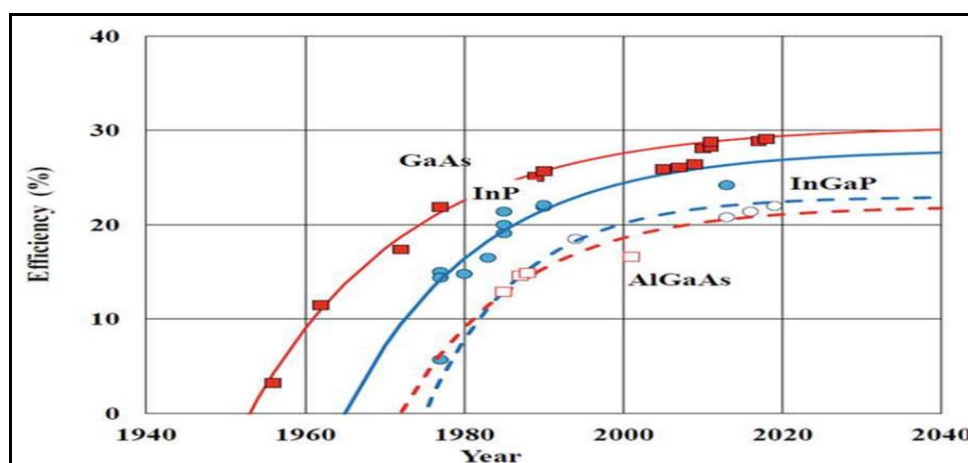


Fig 1 World Record Efficiencies of Single-Junction III-V Compound Materials Under 1-Sun [1].

Despite these advantages, GaAs photovoltaics face some challenges. First, like any crystalline material, GaAs is susceptible to surface recombination, particularly at the collection of the photocurrent. Secondly, as shown on Fig. 2

by Gennady [2], the optical reflectance of GaAs is relatively high, particularly in the visible spectrum where GaAs is anticipated to optimize conversion. This directly affects the quantum efficiency of GaAs.

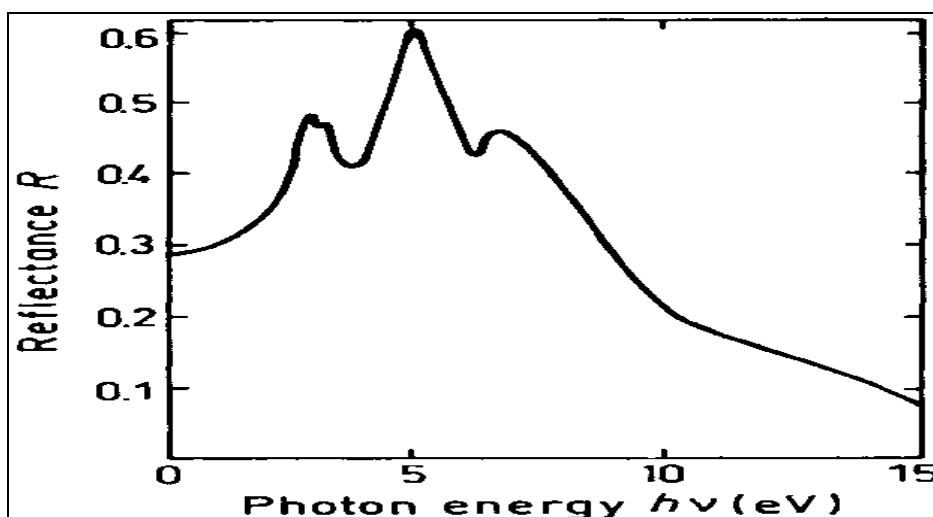


Fig 2 Normal Incidence Reflectivity of the GaAs Versus Photon Energy [2]

In relation to the issue with the surface recombination, two main techniques categories can be adopted to reduce the recombination rate for an optimal performance. These include surface treatment and surface passivation.

Several common techniques are used for surface treatment such as chemical passivation, thermal annealing, plasma treatment, etching and oxidation. These techniques can reduce the number of surface states at the interface. However, they may not be sufficient to lower the concentrations of surface recombination sites and mitigate the effects of grain boundary. Furthermore, their effectiveness can sometimes be temporary as surface states may reappear over time. Gennady [2] illustrated this limitation with Fig. 3, where he shows the recombination rate versus doping density for GaAs using different surface treatment techniques. As observed, the lowest recorded recombination rate, regardless of the surface treatment technique applied, is approximately 10^5 cm/s for a doping density of 10^{16} cm $^{-3}$. For a doping density of 10^{17} cm $^{-3}$, the recombination rate increases to 10^6

cm/s. These values are still relatively high, significantly impacting the overall performance of the solar cell.

Surface passivation techniques involve the application of an additional layer with a gradual bandgap, as well as the utilization of a double heterostructure. These methods not only reduce surface recombination, but it also serves to protect the solar cell against harsh environment conditions, radiation and minimize light reflection. An ideal solar cell must be able to absorb over 98% of useful photons (from incident light) to generate electrical charges and high photocurrent.

While both surface treatment and surface passivation techniques address issues related to surface recombination, they aim different aspects of this problem. Therefore, they are often combined to enhance overall performance. However, in this article, we will place greater emphasis on the surface passivation technique, particularly on window layering technique.

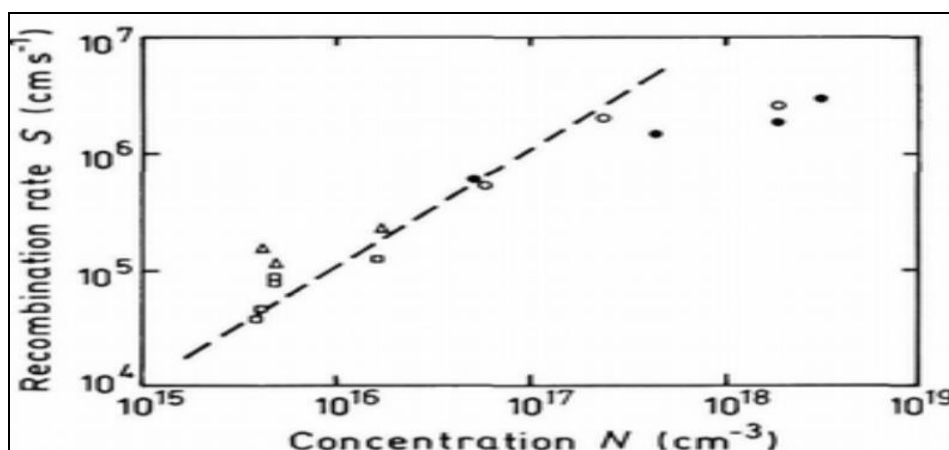


Fig 3 Surface Recombination Velocity Versus Doping Density for GaAs. Different Experimental Points Correspond to Different Surface Treatment Technique [2]

For GaAs-based solar cells, single layer of Aluminum Gallium Arsenide (AlGaAs) and Gallium Indium Phosphide (GaInP) are extensively studied and used. This article offers a comparative study of $\text{Al}_{0.8}\text{Ga}_{0.2}\text{As}$ and $\text{Ga}_{0.51}\text{In}_{0.49}\text{P}$ window layers for GaAs-based solar cells. Several publications on similar topics have been issued, each with its own pros and cons.

Reference [3] compared the performance of two cells that use two different window layers: $\text{Al}_{0.2}\text{Ga}_{0.8}\text{As}$ and $\text{Ga}_{0.51}\text{In}_{0.49}\text{P}$. Both structures were simulated with SCAPS-1D. The study focused on optimizing both structures separately to find the optimal values for thickness and doping density before comparing their performance. The study concluded that $\text{Ga}_{0.51}\text{In}_{0.49}\text{P}$ with a thickness of 0.1 μm performed better, with a maximum efficiency of 25.02%. Despite of its clear method of comparison, the study omits some crucial parameters that affect the performance of the solar cell. Firstly, it neither mentions nor provides the values of the lattice constants for the window layer materials. Lattice matching is very important in reducing the recombination. Secondly, optical parameters such as transmittance and refractive index were overlooked, even though they directly affect quantum efficiencies. Lastly, the study did not provide an analytical model of the surface recombination and light reflection, which is essential for identifying the parameters that must be considered.

Similarly, Reference [6] demonstrated the contribution of window layer $\text{Al}_{0.8}\text{Ga}_{0.2}\text{As}$ in the overall performance of the GaAs-based solar cell. The simulation was carried out using SCAPS-1D, and the results reported a noticeable increase in efficiency from 17.23% to 27.23%. The authors concluded that the window layer should be very thin (20 nm) and slightly doped ($2 \times 10^{18} \text{ cm}^{-3}$) to achieve good performance. Although the article showed promising results, it did not account for critical parameters such as surface

recombination velocity and bulk recombination, casting doubt on the findings.

Reference [5] have proposed the use of Cadmium Sulfide (CdS) as window layer to reduce de surface recombination for GaAs. CdS is a direct bandgap semiconductor of 2.41 eV, and it exhibits good optical transmittance. However, the use of CdS must be done carefully due to the toxicity of the Cadmium, making it not an ideal candidate as a window layer.

This article aims to complement previous studies by considering a broader range of parameters such as surface recombination velocity and minority carrier lifetime and optimizing separately each candidate window layer before comparison. Additionally, it also provides some analytical models to understand further the relevance of each parameter. Finally, it utilizes PC1D for numerical simulation. All these efforts are directed towards offering a clear and concise comparison of the candidate materials for better performance while ensuring safety, cost-effective and environmental friendliness.

II. MATERIALS AND METHODS

➤ Structure of Solar Cell Alta Device 2012.05

The comparison of both window layers is conducted on a solar cell Alta Device 2012.05, as provided by Chaomin Zhang [7]. It is a single-junction GaAs solar cell fabricated by Alta Device company. Its base is made of n-GaAs with a thickness of 1.5 μm and a doping density of $2 \times 10^{17} \text{ cm}^{-3}$, while its emitter is made of p-GaAs with thickness of 0.15 μm and a doping density of $1 \times 10^{18} \text{ cm}^{-3}$. The BSF layer is made of n-GaAs with a thickness of 0.02 μm and a doping density of $4 \times 10^{18} \text{ cm}^{-3}$. The original window layer of the Alta Device is made of $\text{Al}_{0.85}\text{Ga}_{0.15}\text{As}$ with a doping density of $3 \times 10^{18} \text{ cm}^{-3}$. This will be replaced with $\text{Al}_{0.2}\text{Ga}_{0.8}\text{As}$ and $\text{Ga}_{0.51}\text{In}_{0.49}\text{P}$ in this study.

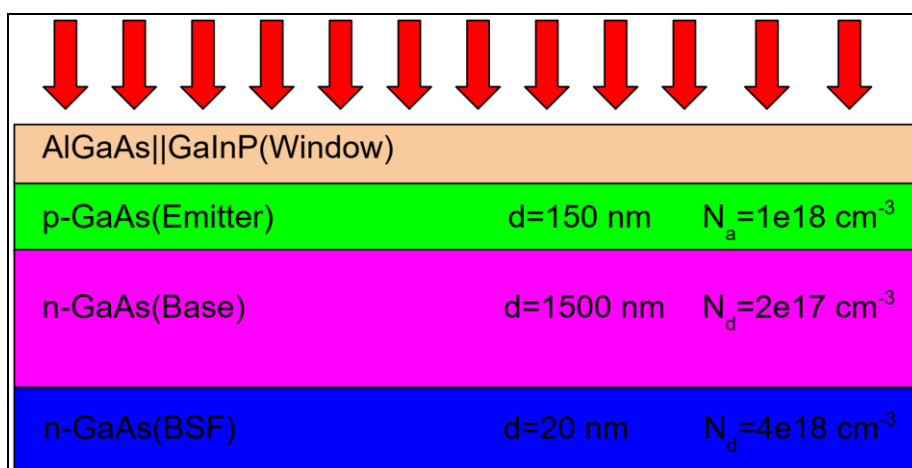


Fig 3 Basic Structure of the Alta Device 2012.05 Solar Cell Simulated in this Study

➤ Numerical simulation

PC1D has been chosen for the numerical simulation of the structure shown in Fig. 3. It is a one-dimensional solar cell simulation and was developed and maintained at University of Sydney. The program is free of charge and its raw code is

available to programmers and developers for customization. It can simulate single to multi-junction solar cells and provide various electrical and quantum characteristics. Amongst of those characteristics include doping densities, carrier density, electrostatic potential, electric field, charge density, current

density, generation & recombination, carrier mobilities, energy bands, carrier velocities, diffusion length, base I-V / Power, base current, base voltage, quantum efficiency etc... All this information is calculated by PC1D based on the fundamental equations of semiconductors which are the transport equation, the continuity equation and the Poisson's equation.

➤ Material Properties for GaAs

PC1D integrates most of the properties for GaAs, which are reported in Table 1. In addition, surface recombination velocity and minority carrier lifetime must be specified.

The surface recombination velocity defines the surface recombination flux as per the equation provided by Jenny [9]:

$$U_s \delta x \approx S_n (n_s - n_0) \quad (1)$$

Where:

Table 1 Main Materials Properties for GaAs Absorber and Substrate at 300°K

	Emitter p-GaAs	Base n-GaAs	Substrate n-GaAs
Bandgap (eV)	1.424	1.424	1.424
Thickness (μm)	0.15	1.5	0.02
Electron affinity (eV)	4.07	4.07	4.07
Dielectric permittivity (relative)	13.18	13.18	13.18
Ratio Nc/Nv	0.034	0.034	0.034
Electron mobility (cm ² /Vs)	8569	8569	8569
Hole mobility (cm ² /Vs)	408	408	408
Donor density (cm ⁻³)	1x10 ¹⁸	-	-
Acceptor density (cm ⁻³)	-	2x10 ¹⁷	4x10 ¹⁸
Intrinsic conc. (10 ⁶ cm ⁻³)	2.59	2.59	2.59
Lifetime (μs)	0.005	3	3

For the candidate window layers, material properties are determined either analytically using Vegar's law or through empirical data.

➤ Lattice Parameter

Lattice constant is a critical parameter for window layering because lattice mismatch directly affects the performance and reliability of a solar cell. Lattice mismatch is calculated with:

$$\Delta \equiv \frac{|a_e - a_s|}{a_e} \quad (2)$$

where a_e and a_s are the lattice constants of the epitaxial layer and substrate respectively. Milton wrote that optical a lattice mismatch of less than 0.1% is sought for optical devices [10].

Lattice parameter obeys to Vegar's law. Reference [11] provides the equations for both candidate window layer materials. For $\text{Al}_x\text{Ga}_{1-x}\text{As}$, the equation is given by:

$$a = 5.6533 + 0.0078x \quad (3)$$

- S_n = surface recombination velocity, which is a material and technology-dependent parameter. The best record on S_n in GaAs, after applying surface treatment technique, is 100 cm/s according to Ekins-Daukes et al. [8].
- n_s = concentration of excess electrons at the interface. Its value is given by the expression $e^{\frac{q\Phi_s}{k_B T}}$, where Φ_s is the surface potential, which can be found by solving Poisson's equation. That can be only achieved using numerical method due to the non-linearity of the equation, hence the use of simulation programs.

As for the minority carrier lifetime, it is required to calculate the bulk recombination, which is involved in continuity equation. This calculation is required to determine the carrier density in Poisson's equation. The values reported in Table 1 are obtained from Gennady et al. [2]

The lattice parameter of $\text{Al}_{0.2}\text{Ga}_{0.8}\text{As}$ can be calculated as 5.65486 Å. This value closely matches that of GaAs (5.65325 Å) with only a 0.02% of mismatch when calculated using (3).

Similarly, for $\text{Ga}_x\text{In}_{1-x}\text{P}$, the lattice parameter is calculated using the equation:

$$a = 5.8687 - 0.4182x \quad (4)$$

For a molar composition of $x=0.51$, the lattice parameter for $\text{Ga}_{0.51}\text{In}_{0.49}\text{P}$ is calculated as 5.655418 Å, which is even closer to that of GaAs with only 0.01% of mismatch.

To sum up, both materials allow for lattice matching with GaAs, minimizing the density of defects at the interface.

➤ Bandgap

The bandgap is as much as critical because it defines the upper limit of electromagnetic wavelength that a material can absorb, as described by the equation provided by Neamen Donald A. [12]:

$$\lambda = \frac{hc}{E_g} = \frac{1.24}{E_g} \quad (5)$$

Like lattice parameter, the alloy's bandgap calculation abides by Vegar's law. The equations for both candidate window layers are provided on MSN. For $\text{Al}_x\text{Ga}_{1-x}\text{As}$, the equation for the bandgap is as follows:

$$E_g = 1.424 + 1.247x, \quad x < 0.45 \quad (6)$$

For a molar composition of $x = 0.2$, the bandgap of $\text{Al}_{0.2}\text{Ga}_{0.8}\text{As}$ is calculated to be 1.6734 eV. Using equation (5), it can absorb wavelengths up to 741 nm and will transmit those beyond to GaAs. For GaAs with bandgap 1.424 eV, the upper wavelength limit is 870 nm.

For $\text{Ga}_x\text{In}_{1-x}\text{P}$, the bandgap is given by the equation:

$$E_g = 2.26x + 1.35(1-x) + 0.6x(1-x) \quad (7)$$

Using equation (7), the bandgap for $\text{Ga}_{0.51}\text{In}_{0.49}\text{P}$ is calculated to be 1.664 eV, which corresponds to an upper wavelength limit of 745 nm.

In summary, both candidate window layers exhibit wider bandgap allowing light transmission to the GaAs layer.

➤ Carrier Mobility

In addition to light management, window layer also serves to enhance the current collection. To achieve this, it requires good electrical properties, which rely on carrier mobility according to the fundamental equation of transport.

Carrier mobility for electrons is generally higher than that of holes. Reference [11] provides the equations for both candidate materials.

For $\text{Al}_x\text{Ga}_{1-x}\text{As}$, the equations for electron and hole mobility are respectively:

$\mu_n = 8 \times 10^3 - 2.2 \times 10^4 x + 10^4 x^2, \quad x < 0.45$	(8)
$\mu_p = 370 - 970x + 740x^2$	(9)

Using equation (8) and (9), electron mobility for $\text{Al}_{0.2}\text{Ga}_{0.8}\text{As}$ is calculated to be $4 \times 10^3 \text{ cm}^2\text{V}^{-1}\text{s}^{-1}$ and hole mobility is $205.6 \text{ cm}^2\text{V}^{-1}\text{s}^{-1}$.

For $\text{Ga}_x\text{In}_{1-x}\text{P}$, the electron and hole mobilities are taken from empirical values from NSM [11].

➤ Thickness

Electrical and optical aspects must be considered all together when determining the thickness of the window layer.

Firstly, from electrical perspective, the thickness of the window directly influences the surface potential Φ_s according to Poisson's equation, and consequently the surface carrier density n_s as per Boltzmann's approximation. On one hand, a window layer that is too thick increases the resistance, thereby decreasing the electrical characteristic quality. On the other hand, a layer that is too thin neither provides sufficient surface potential to assist in current collection nor offers effective surface passivation. The determination of minimum thickness depends on the material quality.

Secondly, in terms of optical perspective, the thickness must allow a desirable transmittance of light of at least 85% across a large part of the visible spectrum range (380-750 nm), where GaAs is expected to make the most gain. In fact, an excessively thick window layer reduces light transmittance according to Beer-Lambert law. As illustrated in the Fig. 4 by Jenny Nelson [9], incident light with intensity I_s and reflection R , passing through a semiconductor with thickness x and absorption coefficient α , is attenuated as shown by the thin line.

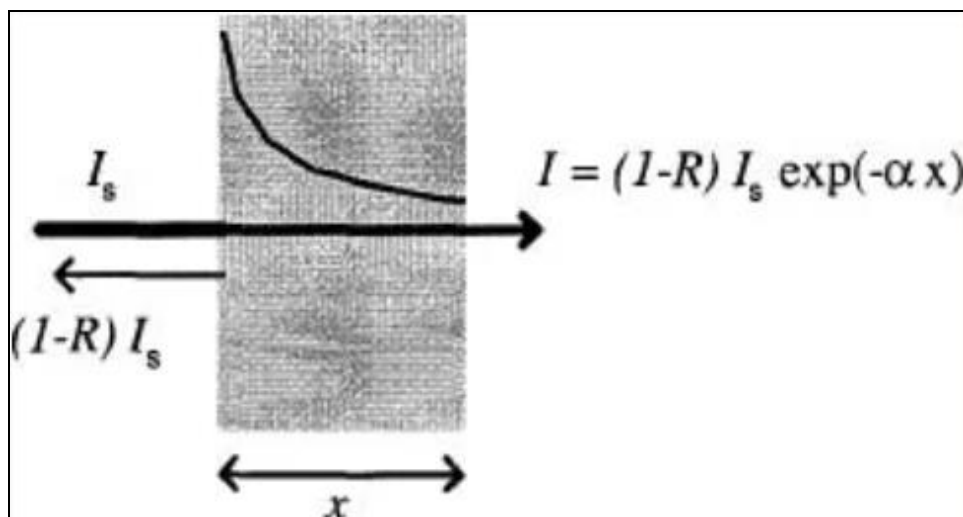


Fig 4 Attenuation of Light Intensity in a Semiconductor According to Beer-Lambert Law

To ensure the desirable transmittance for $\text{Al}_{0.2}\text{Ga}_{0.8}\text{As}$ window layer, the maximum thickness is 70 nm, which provides a transmittance of 86% at a wavelength of 730 nm, as shown by Fig. 5. This value represents the upper limit of

the thickness. Regarding the lower limit, it can go as low as 10 nm, which allows 86% of transmittance at a wavelength of 475 nm according to Fig. 6.

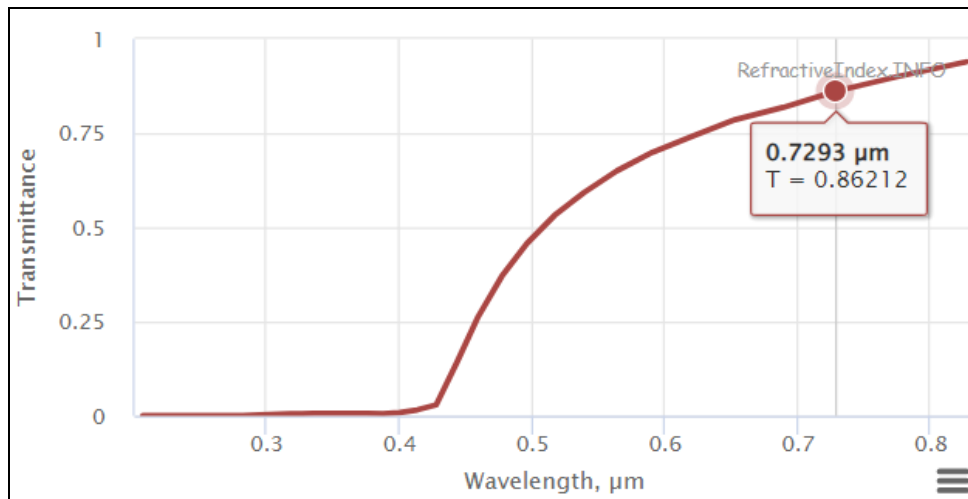


Fig 5 Transmittance of AlGaAs Across the Spectrum Range for a Thickness of 70 nm [11].

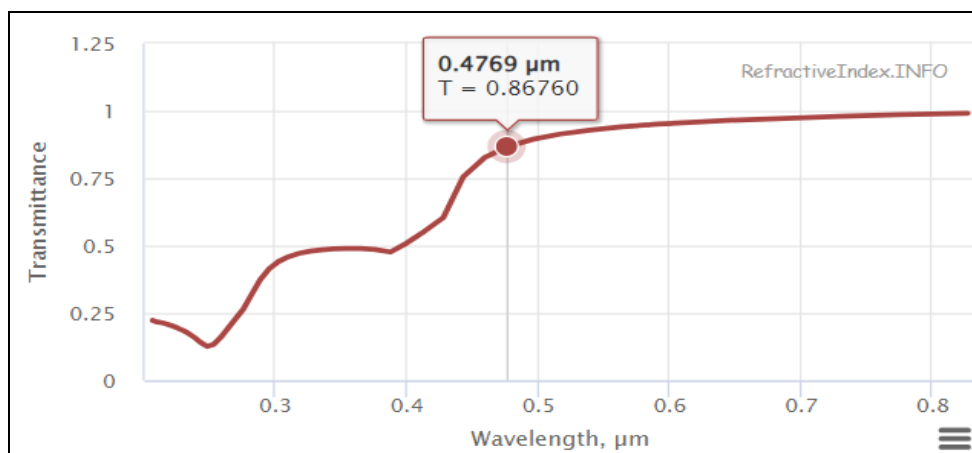


Fig 6 Transmittance of AlGaAs Across the Spectrum Range for a Thickness of 10 nm [11].

$\text{Ga}_{0.51}\text{In}_{0.49}\text{P}$ exhibits better optical properties than $\text{Al}_{0.2}\text{Ga}_{0.8}\text{As}$. In fact, as shown by Fig. 7, it has a

transmittance of 87% at wavelength 673 nm with a thickness 1.5 μm . The lower limit can be the same as $\text{Al}_{0.2}\text{Ga}_{0.8}\text{As}$.

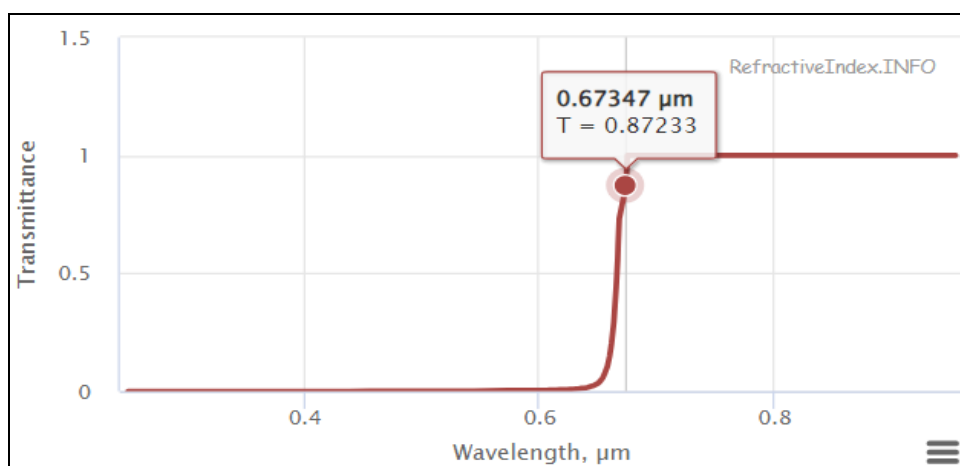


Fig 7 Transmittance of GaInP Across the Spectrum Range for a Thickness of 1 μm .

➤ Doping Density

The orientation of the band diagram across the solar cell must help the movement of the minority carriers to their respective direction. To achieve that on the window layer level, the lower limit of the doping density is that of emitter layer to avoid creating potential barrier to the electrons. For

the upper limit, it is defined by the desirable maximum of resistivity. The resistivity is given by the equation:

$$\rho = \frac{1}{q \cdot N_d \cdot \mu_n} \quad (10)$$

In this study, the maximum value of $\rho=10^{-4} \Omega.\text{cm}^{-1}$ is chosen. To achieve this for $\text{Al}_{0.2}\text{Ga}_{0.8}\text{As}$ window layer, the maximum doping density is $1.5 \times 10^{19} \text{ cm}^{-3}$ when calculated using (10). For $\text{Ga}_{0.51}\text{In}_{0.49}\text{P}$ window layer, the upper limit of the doping density is $1.7 \times 10^{20} \text{ cm}^{-3}$.

To recap, main material properties for both candidate windows layers are summarized on Table 2. Properties such as electron affinity, dielectric permittivity, carrier mobilities, surface recombination velocity, and intrinsic concentration are taken from NSM [11]. The remaining parameters are typical values.

Table 2 Main Materials Properties for Candidate Window Layers at 300°K

	$\text{Al}_{0.2}\text{Ga}_{0.8}\text{As}$	$\text{Ga}_{0.51}\text{In}_{0.49}\text{P}$
Thickness (nm)	10-70	10 – 1500
Bandgap (eV)	1.673	1.664
Electron affinity (eV)	3.85	4.1
Dielectric permittivity (relative)	12.332	11.8
Ratio N_c/N_v	0.05	0.046
Electron mobility (cm^2/Vs)	4000	350
Hole mobility (cm^2/Vs)	205.6	75
Acceptor density (10^{18} cm^{-3})	1×10^{18} - 1.5×10^{19}	1×10^{18} - 1.7×10^{20}
Absorption coefficient	PC1D-GaAs	105
Refractive Index ¹	PC1D-GaAs	3.58 [13]
Intrinsic conc. (cm^{-3})	2.1×10^6	7.5×10^3
Front-Surface recombination velocity (cm/s)	45	1.5
Minority carrier lifetime (μs)	0.01	0.1

The structure represented by Fig. 3 is simulated on PC1D with the parameters provided in Table 1 and Table 2. The device area is 1 cm^2 with a surface texture depth of 3 μm to reduce the reflection, and shunt resistance of $1 \times 10^{-3} \text{ S}$. The excitation is an AM1.5 solar spectrum with a constant intensity of 0.1 W.cm^{-2} striking the structure in transient mode of 50 timesteps at temperature 300°K. For the determination of electrical characteristics, the base voltage is specifically varied from -0.8 V to 0.8 V.

III. RESULTATS AND DISCUSSIONS

➤ Determination of the Optimal Thickness

For an unbiased comparison between both candidate window layers, the optimal thickness of each is determined separately by varying the value within the range calculated during the analytical process and comparing the maximum base power.

For $\text{Al}_{0.2}\text{Ga}_{0.8}\text{As}$ window layer, the thickness is varied from 10 nm to 70 nm by stepping up 20 nm every time. As can be seen on Fig. 8, the maximum base power is obtained for a thickness of 10 nm.

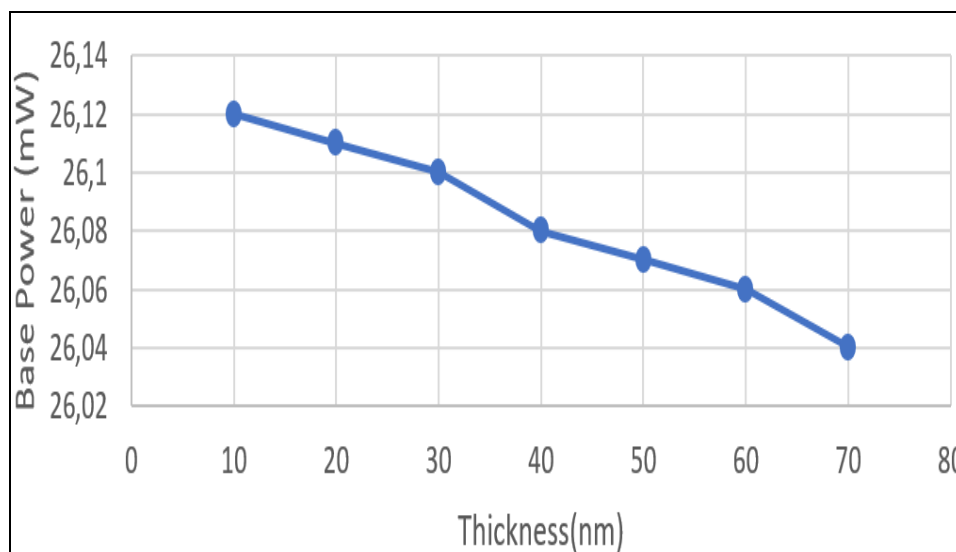


Fig 8 Base Power for Different Thickness of $\text{Al}_{0.2}\text{Ga}_{0.8}\text{As}$ Window Layer

Similarly, for $\text{Ga}_{0.51}\text{In}_{0.49}\text{P}$ window layer, the thickness is incremented from 10 nm to 1.5 μm with a step of 100 nm.

As can be observed on Fig. 9, the thickness 1.2 μm delivers the highest base power.

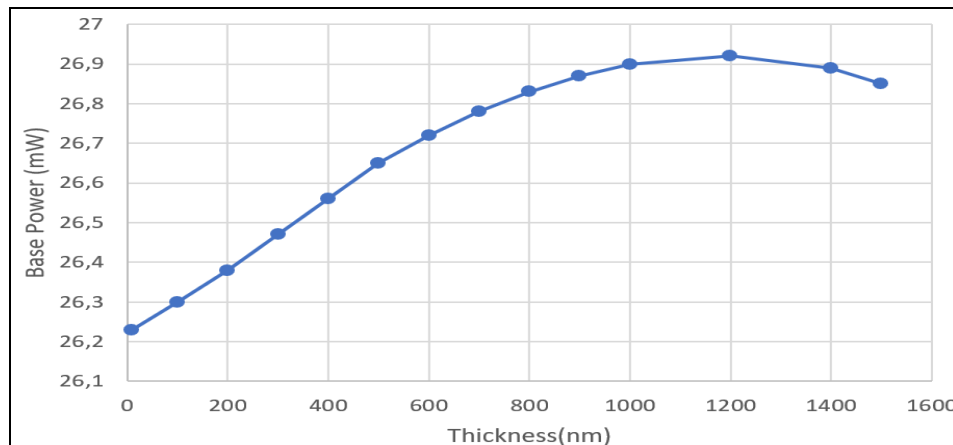


Fig 9 Base Power for Different Thickness of Ga_{0.51}In_{0.49}P Window Layer

In summary, Ga_{0.51}In_{0.49}P allows thicker window layer compared to Al_{0.2}Ga_{0.8}As. This is because of its better optical properties.

➤ Determination of the Optimal Doping Density

Similar to the thickness, the optimal doping density of each candidate window layer is determined separately.

For the Al_{0.2}Ga_{0.8}As window layer, the doping density is gradually increased from $1 \times 10^{18} \text{ cm}^{-3}$ to $1.5 \times 10^{19} \text{ cm}^{-3}$. As shown in the Fig. 10, the optimal doping density is $1 \times 10^{18} \text{ cm}^{-3}$.

For the Ga_{0.51}In_{0.49}P window layer, the doping density range is larger, from $1 \times 10^{18} \text{ cm}^{-3}$ to $1.7 \times 10^{20} \text{ cm}^{-3}$. Fig. 11 shows the maximum base power for different doping densities. As can be observed, the highest performance of 26.93 mW is obtained with a doping density of $1 \times 10^{18} \text{ cm}^{-3}$.

For the Ga_{0.51}In_{0.49}P window layer, the doping density range is larger, from $1 \times 10^{18} \text{ cm}^{-3}$ to $1.7 \times 10^{20} \text{ cm}^{-3}$. Fig. 11 shows the maximum base power for different doping densities. As can be observed, the highest performance of 26.93 mW is obtained with a doping density of $1 \times 10^{18} \text{ cm}^{-3}$.

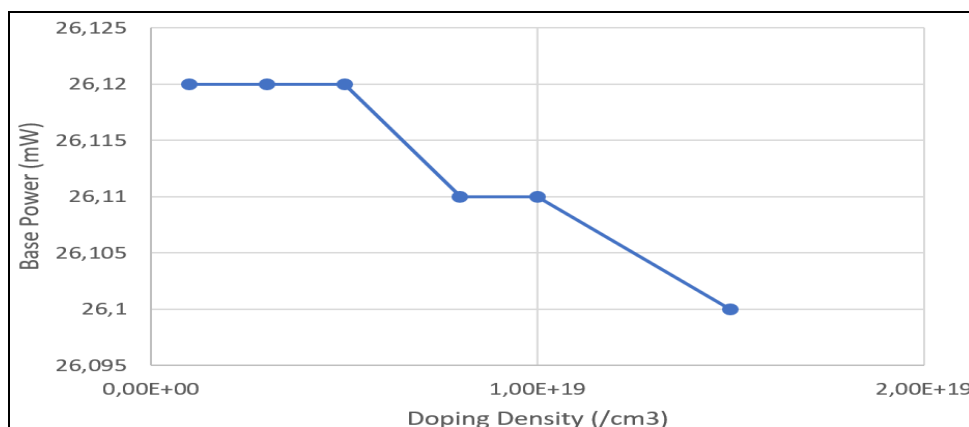


Fig 10 Base Power for Different Doping Density of Al_{0.2}Ga_{0.8}As Window Layer.

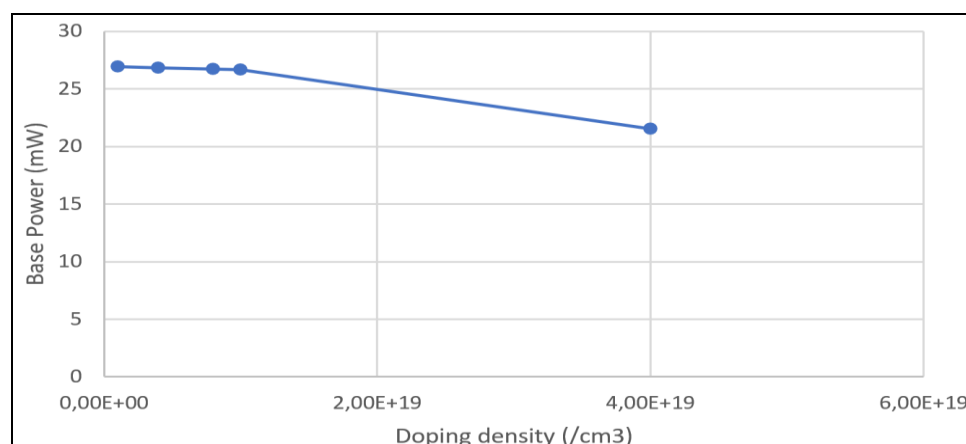


Fig 11 Base Power for Different Doping Density of Ga_{0.51}In_{0.49}P Window Layer.

To sum up, both candidate materials have the same optimal doping density of $1 \times 10^{18} \text{ cm}^{-3}$.

➤ Comparison of IV Characteristics

Having determined the optimal values for thickness and doping density for each candidate materials, an equitable comparison can be conducted.

The IV curves for $\text{Al}_{0.2}\text{Ga}_{0.8}\text{As}$ and $\text{Ga}_{0.51}\text{In}_{0.49}\text{P}$ window layers are shown in Fig. 12. As can be seen, the structure with $\text{Ga}_{0.51}\text{In}_{0.49}\text{P}$ delivers an overall better result

compared to $\text{Al}_{0.2}\text{Ga}_{0.8}\text{As}$ window layer. The short-circuit current J_{sc} is higher by 0.21 mA/cm^2 , the open-circuit potential V_{oc} is up by 0.0236 V and the maximal base power is greater by 0.51 mW/cm^2 . The fill factor is slightly lower, by 0.77% .

The difference of 0.51 mW/cm^2 on the base power represents approximately 2.55% of the total output. This is generally significant, especially in competitive markets or high-precision applications where maximum performance is essential.

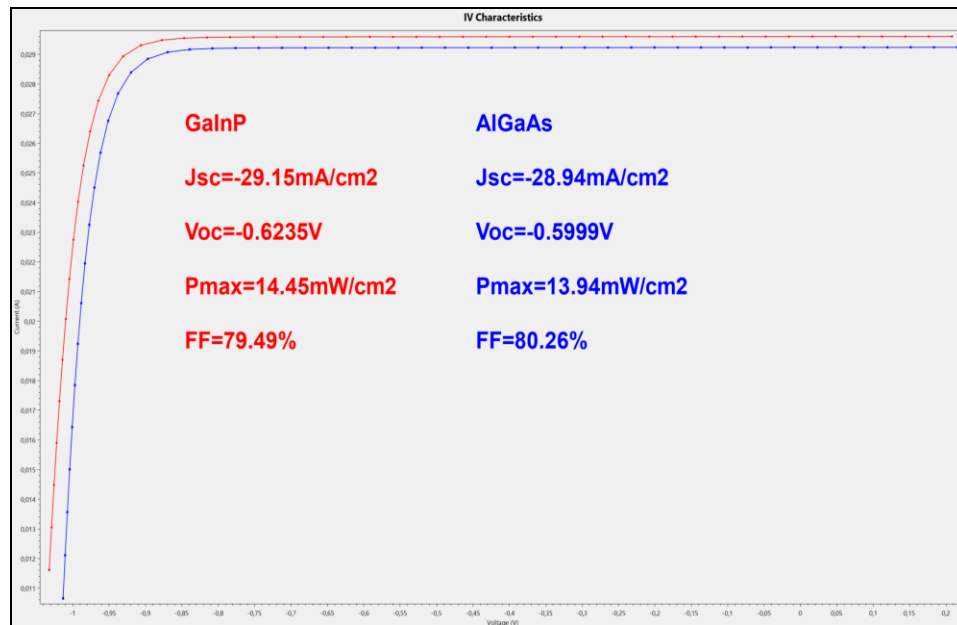


Fig 12 IV Curves for $\text{Ga}_{0.51}\text{In}_{0.49}\text{P}$ and $\text{Al}_{0.2}\text{Ga}_{0.8}\text{As}$ Window Layers

➤ Internal Quantum Efficiency

To further analyze the origin of the better performance of the structure with $\text{Ga}_{0.51}\text{In}_{0.49}\text{P}$ window layer, the internal quantum efficiency (IQE) for both window materials is compared on Fig. 13. As can be observed, the IQE for

$\text{Ga}_{0.51}\text{In}_{0.49}\text{P}$ is higher by approximately 2% in the range of visible spectrum. To determine the significance of this finding on performance, further analysis of photogeneration is required.

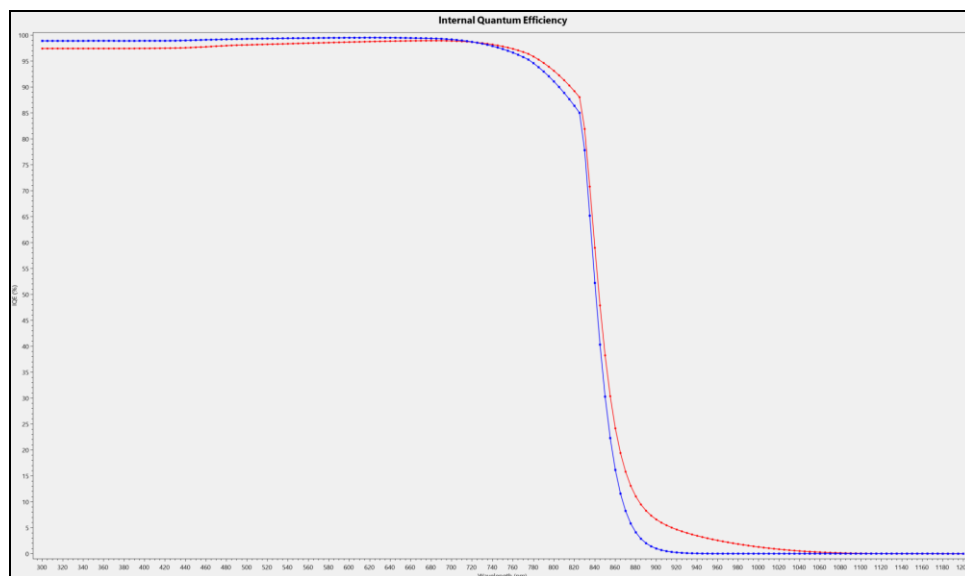


Fig 13 Internal Quantum Efficiency (IQE) Versus Wavelength for $\text{Ga}_{0.51}\text{In}_{0.49}\text{P}$ (Red) and $\text{Al}_{0.2}\text{Ga}_{0.8}\text{As}$ (Blue) Window Layers

➤ Photogeneration

The Fig. 14 and Fig. 15 represent the cumulative photogeneration versus distance from front for $\text{Al}_{0.2}\text{Ga}_{0.8}\text{As}$ and $\text{Ga}_{0.51}\text{In}_{0.49}\text{P}$, respectively. As can be seen, the cumulative generation of both structures is almost the same, with a value

of $1.836 \times 10^{17} \text{ s}^{-1}$ for $\text{Al}_{0.2}\text{Ga}_{0.8}\text{As}$, and $1.837 \times 10^{17} \text{ s}^{-1}$ for $\text{Ga}_{0.51}\text{In}_{0.49}\text{P}$. This indicates that the difference in performance is not due to the photogeneration but rather other factor, such as carrier transport. Consequently, an analysis from this perspective is conducted.

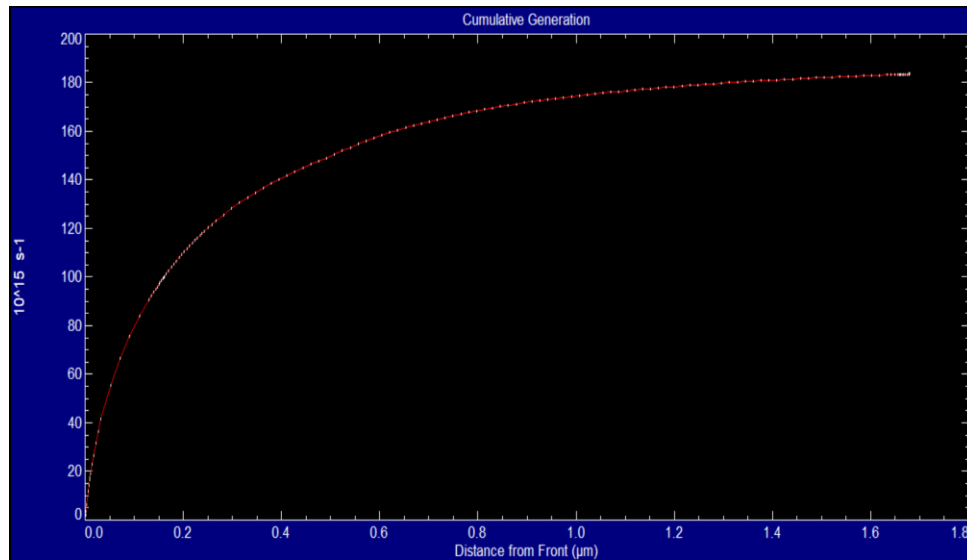


Fig 14 Cumulative Generation Versus Distance from Front for the Structure with $\text{Al}_{0.2}\text{Ga}_{0.8}\text{As}$ Window Layer

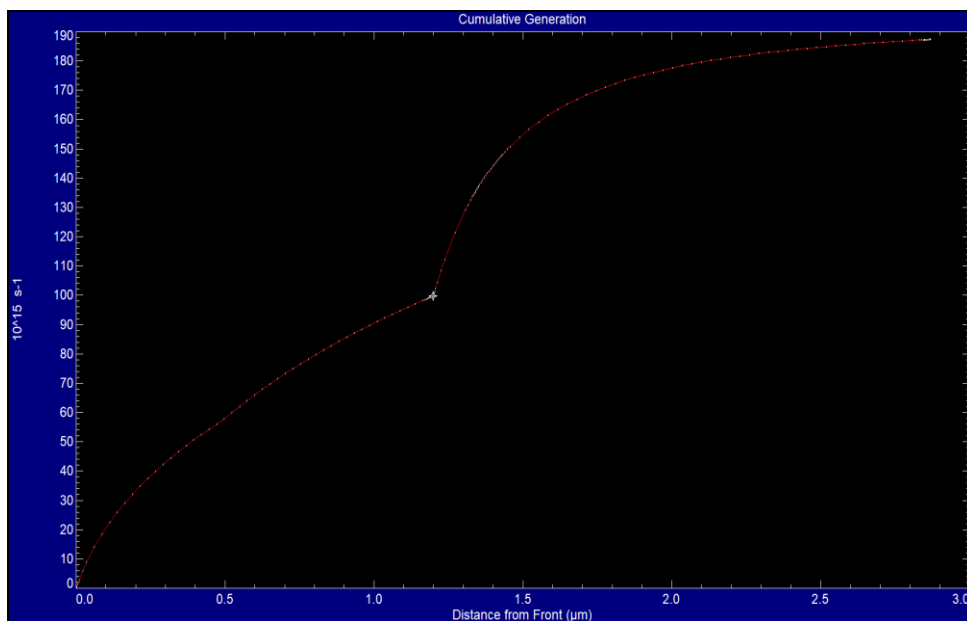


Fig 15 Cumulative Generation Versus Distance from Front for the Structure with $\text{Ga}_{0.51}\text{In}_{0.49}\text{P}$ Window Layer.

➤ Electric Field

The electric field in the depletion region helps separate the photo-generated electron-hole pairs, driving electrons towards n-type side and holes towards the p-type side. Therefore, the direction and the magnitude of electrical field inside the depletion region are critical for the carrier transport.

Firstly, in terms of the direction, for the structure represented on Fig. 3, a positive value of electric field indicates that the electric field vector is pointing from the window layer to the emitter, opposing the direction of photo-

generated current. This is the case for the structure with $\text{Al}_{0.2}\text{Ga}_{0.8}\text{As}$ as being shown by Fig. 16 around the interface between the window layer and the emitter. In contrast, the electric field for structure with $\text{Ga}_{0.51}\text{In}_{0.49}\text{P}$ is negative around the depletion region according to Fig. 17, aiding carrier transport.

Secondly, in terms of magnitude, a strong electric field in the correct direction allows for better electrical performance. According to Fig. 17, the $\text{Ga}_{0.51}\text{In}_{0.49}\text{P}$ structure provides a high electrical field of -234.5 kV/cm.

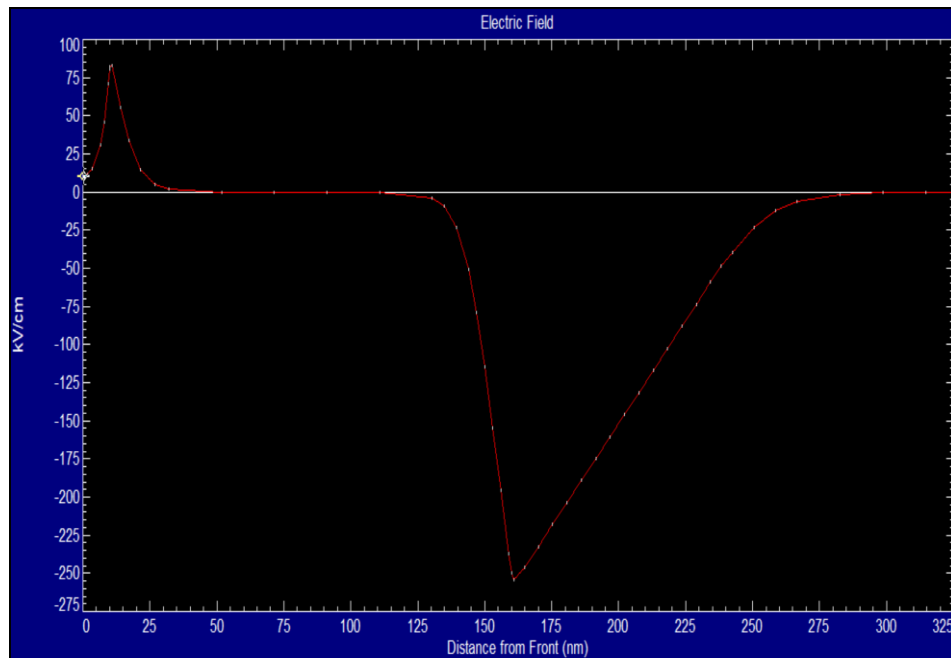


Fig 16 Electric Field Versus Distance from Front for the Structure with $\text{Al}_{0.2}\text{Ga}_{0.8}\text{As}$ Window Layer.

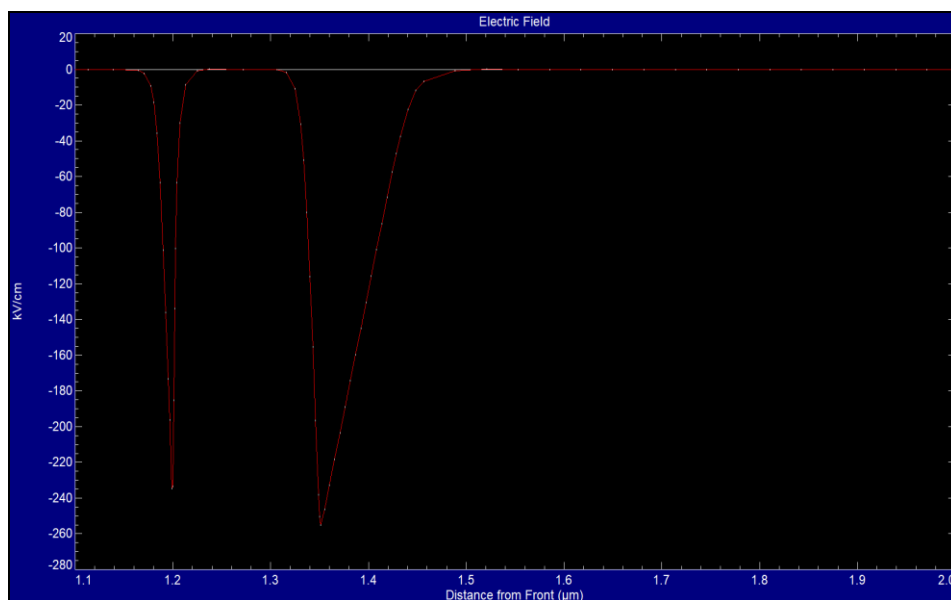


Fig 17 Electric Field Versus Distance from Front for the Structure with $\text{Ga}_{0.51}\text{In}_{0.49}\text{P}$ Window Layer.

In summary, the difference the two structures lies in the transport of the photocurrent. $\text{Ga}_{0.51}\text{In}_{0.49}\text{P}$ provides better transport properties due to its high optical transmittance, which allows thicker window layer and a stronger electric field.

IV. CONCLUSION

In this work, $\text{Al}_{0.2}\text{Ga}_{0.8}\text{As}$ and $\text{Ga}_{0.51}\text{In}_{0.49}\text{P}$ were simulated as window layers using PC1D for the Alta-Device 2012.05 solar cell structure to determine the most suitable material.

First, each of candidate window layer was optimized separately to determine its optimal thickness and doping density. It was found that the optimal thicknesses for $\text{Al}_{0.2}\text{Ga}_{0.8}\text{As}$ and $\text{Ga}_{0.51}\text{In}_{0.49}\text{P}$ are 10nm and 1.2 μm , respectively. For the doping density, both materials showed best performance at $1 \times 10^{18} \text{cm}^{-3}$.

Then, the IV characteristics were compared and analyzed. The result demonstrated that $\text{Ga}_{0.51}\text{In}_{0.49}\text{P}$ provides better results than $\text{Al}_{0.2}\text{Ga}_{0.8}\text{As}$ in most of merit figures the open-circuit voltage, the maximum base power, and the short-circuit current are higher. A deeper analysis revealed that these results are due to the better optical response and stronger electric field for $\text{Ga}_{0.51}\text{In}_{0.49}\text{P}$.

ACKNOWLEDGMENT

Special thanks to my supervisor, Pr. Elisée Rastefano for his valuable guidance, encouragement, and dedication throughout my Bachelor's, Master's, and now doctoral study.

I am also grateful to my son Emilio Rasoloniaina, who aspires to become an astrophysicist. His great dream inspires me to complete my doctoral studies and set a good example for our family.

REFERENCES

- [1]. Masafumi Yamagushi. High-Efficiency GaAs-Based Solar Cells. Intechopen. <https://www.intechopen.com/chapters/73981>. Published 09 November 2020. 2020. Accessed 10 August 2025.
- [2]. Gennady Sh Gildenblat, Yu A Goldberg, Michael E Levinshtein. Handbook Series On Semiconductor Parameters. Vol. 1: Si, Ge, C (Diamond), GaAs, Gap, Gasb, InAs, InP, InSb. World Scientific; 1996.p.93.
- [3]. BOURBARA H., KADRI S., DJERMANE K. Optimization of the solar cell GaAs: Effect of window layer. Journal of Ovonic Research Vol.15. 2019.
- [4]. Cedrik Fotcha Kamdem, Auriel Teyou Ngoupo, Francisco Kouadio Kona, Herve Joel Tchognia Nkuissi, Bounchaib Hartiti and Jean-Marie Ndjaka. Study of the Role of Window Layer Al_{0.8}Ga_{0.2}As on GaAs-based Solar Cells Performance. Indian Journal of Science and Technology, Vol 12. 2019.
- [5]. Deb Kumar Shah et al. A computational study of carrier lifetime, doping concentration, and thickness of window layer for GaAs solar cell based on Al₂O₃ antireflection layer. Journal Solar Energy, Vol. 234. 2022.
- [6]. Cedric Fotcha Kamdem et al. Study if the Role of Window Layer Al_{0.8}Ga_{0.2}As on GaAs-based Solar Cells Performance. Indian Journal of Science and Technology, Vol 12(37). 2019.
- [7]. Chaomin Zhang. High Efficiency GaAs-based Solar Cells Simulation and Fabrication. A thesis presented in partial fulfillment of the requirements for the degree Master of Science. 2014.
- [8]. N. R. Ekins-Daukes et al. Surface Passivation of GaAs. Journal of Applied Physics. 2002.
- [9]. Jenny Nelson. The Physics of Solar Cells. ICP. 2003.p.111,89,258,261.
- [10]. Milton Ohring. Materials Science of Thin Films. Academic Press. 2001.p.443
- [11]. NSM (National Semiconductor Metrology). <https://www.ioffe.ru/SVA/NSM/Semicond/>. NSM. Accessed on 08 September 2024.
- [12]. Neamen Donald A. Semiconductor Physics and Devices. Fourth Edition. University of New Mexico. 2003.p.619.
- [13]. Polyanskiy, M. N. Refractiveindex.info database of optical constants. <https://doi.org/10.1038/s41597-023-02898-2>. Accessed on 12 September 2024.
- [14]. Shi Liu et al. MgF₂/ZnS double-layer anti-reflection coating design for ultra-thin GaAs single-junction solar cells. Optics for Solar Energy 2013. 2013.